Original Article

L-distance ratio: a new distance ratio-based evaluation method for the diagnosis of cirrhosis using enhanced computed tomography

Huifen Ye[1,2,3#], Qiushi Wang[2#], Haitao Huang[2,3,4#], Ke Zhao[2,3], Pinxiong Li[1,2,3], Zaiyi Liu[1,2,3], Guangyi Wang[2], Changhong Liang[1,2,3]

[1]The Second School of Clinical Medicine, Southern Medical University, Guangzhou, China; [2]Department of Radiology, Guangdong Provincial People's Hospital (Guangdong Academy of Medical Sciences), Southern Medical University, Guangzhou, China; [3]Guangdong Provincial Key Laboratory of Artificial Intelligence in Medical Image Analysis and Application, Guangzhou, China; [4]School of Medicine, South China University of Technology, Guangzhou, China

Contributions: (I) Conception and design: G Wang, Q Wang, C Liang, Z Liu, H Ye, K Zhao; (II) Administrative support: G Wang, C Liang, Z Liu; (III) Provision of study materials or patients: Q Wang, G Wang, C Liang, Z Liu, P Li; (IV) Collection and assembly of data: H Ye, P Li; (V) Data analysis and interpretation: G Wang, H Ye, K Zhao, H Huang; (VI) Manuscript writing: All authors; (VII) Final approval of manuscript: All authors.

[#]These authors contributed equally to this work.

Correspondence to: Changhong Liang. The Second School of Clinical Medicine, Southern Medical University, 1023 South Shatai Road, Baiyun District, Guangzhou 510515, China. Email: liangchanghong@gdph.org.cn; Guangyi Wang. Department of Radiology, Guangdong Provincial People's Hospital (Guangdong Academy of Medical Sciences), Southern Medical University, 106 Second Zhongshan Road, Guangzhou 510080, China. Email: wangguangyi@gdph.org.cn; Zaiyi Liu. The Second School of Clinical Medicine, Southern Medical University, 1023 South Shatai Road, Baiyun District, Guangzhou 510515, China. Email: liuzaiyi@gdph.org.cn.

Background: Early detection of liver cirrhosis is of great significance to the formulation of treatment plans and improving prognosis. Computed tomography (CT) is commonly used in the assessment of patients with chronic liver disease. In this study, we proposed a new distance ratio method for accurate diagnosis of cirrhosis using CT images.

Methods: This was a retrospective study of a consecutive series of patients in Guangdong Provincial People's Hospital. Sixty-two patients with pathologically diagnosed cirrhosis but whose morphologic changes were insufficient to diagnose cirrhosis were included in the cirrhosis group. Those who were pathologically confirmed to be free of cirrhosis and fibrosis and without a history of chronic hepatic were classified as the control group. A total of 124 patients underwent abdominal dynamic enhanced CT. Both the L-distance ratio—the ratio of the distance from the right portal vein bifurcation point to the anterior and posterior edges of the liver—and the caudate-right lobe ratio were measured by two independent radiologists. Intraclass correlation coefficients (ICCs) were used to assess the agreement between the radiologists. Binary logistic regression was performed for univariate analysis, and the odds ratio (OR) was also calculated. The discrimination ability of the two methods was evaluated by the area under the receiver operating characteristic curve (AUC).

Results: For both the L-distance ratio and the caudate-right lobe ratio, high agreement was observed between the two radiologists, although the ICC value of the L-distance ratio was slightly higher than that of the caudate-right lobe ratio (0.916 *vs.* 0.907). Binary logistic regression suggested that higher ratios were correlated with cirrhosis [the L-distance ratio, high *vs.* low OR =4.41, 95% confidence interval (CI): 2.08–9.36, P<0.001; the caudate-right lobe ratio, high *vs.* low OR =2.19, 95% CI: 1.07–4.49, P=0.031]. The AUCs of the L-distance ratio and the caudate-right lobe ratio were 0.823 (95% CI: 0.752–0.894) and 0.663 (95% CI: 0.569–0.757), respectively.

Conclusions: The L-distance ratio method proposed in this paper is more simple, accurate, and reliable than the caudate-right lobe ratio method in the diagnosis of cirrhosis.

Keywords: The L-distance ratio; cirrhosis; diagnosis; the caudate-right lobe ratio; liver

Submitted Aug 15, 2022. Accepted for publication Dec 14, 2022. Published online Jan 09, 2023.
doi: 10.21037/qims-22-861
View this article at: https://dx.doi.org/10.21037/qims-22-861

Introduction

Cirrhosis is a significant public health problem. In 2017, the global age-standardized prevalence of compensated and decompensated cirrhosis was 1,395 (1,323–1,470) and 132 [128–136] per 100,000 population, respectively. In the same year, cirrhosis was responsible for more than 1.32 million (95% uncertainty interval, 1.27–1.45) deaths, which represented 2.4% (95% uncertainty interval 2.3–2.6) of all deaths worldwide (1).

The most common etiologies of cirrhosis are chronic viral hepatitis, alcoholism, and non-alcoholic fatty liver disease (2,3). The different etiologies of cirrhosis present with similar progression patterns (4). In China, hepatitis B virus (HBV) infection remains the primary cause of cirrhosis (5-8). The 5-year cumulative incidences of hepatocellular carcinoma increase gradually at different stages of HBV infection (9). Moreover, when a patient progresses to cirrhosis, in addition to treatment to address the cause, steps need to be taken to prevent and reduce complications. Therefore, early detection of liver fibrosis and cirrhosis is of great significance to the formulation of treatment plans and improving prognosis (10).

Several assessment methods have been proposed for the diagnosis of liver fibrosis and cirrhosis, among which liver biopsy is the gold standard for clinical evaluation (11). However, liver biopsy has some limitations, including its invasiveness, the risk of postoperative complications, inconsistencies between and within observers, and the accuracy of the results being easily affected by sampling errors (12-14). Some imaging techniques, such as elastography and magnetic resonance elastography, have the advantages of being non-invasive and reproducible for the evaluation of liver fibrosis and cirrhosis (15,16). To date, there have been many studies on the clinical value of fibroscans and ultrasound (US) elastography in the evaluation of hepatic fibrosis, and vibration-controlled transient elastography is possibly the most widely used technique at present (17). However, the diagnostic ability of computed tomography (CT) was not intended to exceed these methods.

For patients with chronic liver disease who undergo enhanced CT scanning for whatever reason, CT measurement methods can provide radiologists with more comprehensive and additional valuable information. Based on morphological changes of cirrhosis, Awaya *et al.* used the caudate-right lobe ratio—a ratio-based method assessing the right portal vein to set the lateral boundary—to diagnose cirrhosis and reported an area under the receiver operating characteristic (ROC) curve (AUC) of 0.797 (18). However, the cases in their study mainly were alcoholic cirrhosis, whereas HBV infection is the dominant cause of cirrhosis in China (6). Other studies have shown that the proportion of patients with caudate lobe enlargement was significantly higher among those with alcoholic cirrhosis than those with viral cirrhosis (19). Also, the degree of hypertrophy may vary due to differences in the blood supply of the caudate lobe among all populations (20). Therefore, the caudate-right lobe ratio method has poor diagnostic efficacy for cirrhosis. Further, in patients with hepatitis C virus-associated cirrhosis, characteristic changes include shrinkage in the anterior part of the right lobe and enlargement of the posterior segment of the right lobe. We speculated whether these morphological changes are also applicable to patients with other etiologies.

Therefore, in this study, we proposed a new distance ratio measurement method for CT images: the L-distance ratio. We compared the performance of the L-distance ratio with that of the caudate-right lobe ratio in diagnosing cirrhosis. We present the following article in accordance with the STARD reporting checklist (available at https://qims.amegroups.com/article/view/10.21037/qims-22-861/rc).

Methods

Patient population

The study was conducted in accordance with the Declaration of Helsinki (as revised in 2013). This retrospective study was approved by the institutional review board of Guangdong Provincial People's Hospital, and the requirement to obtain individual consent for this

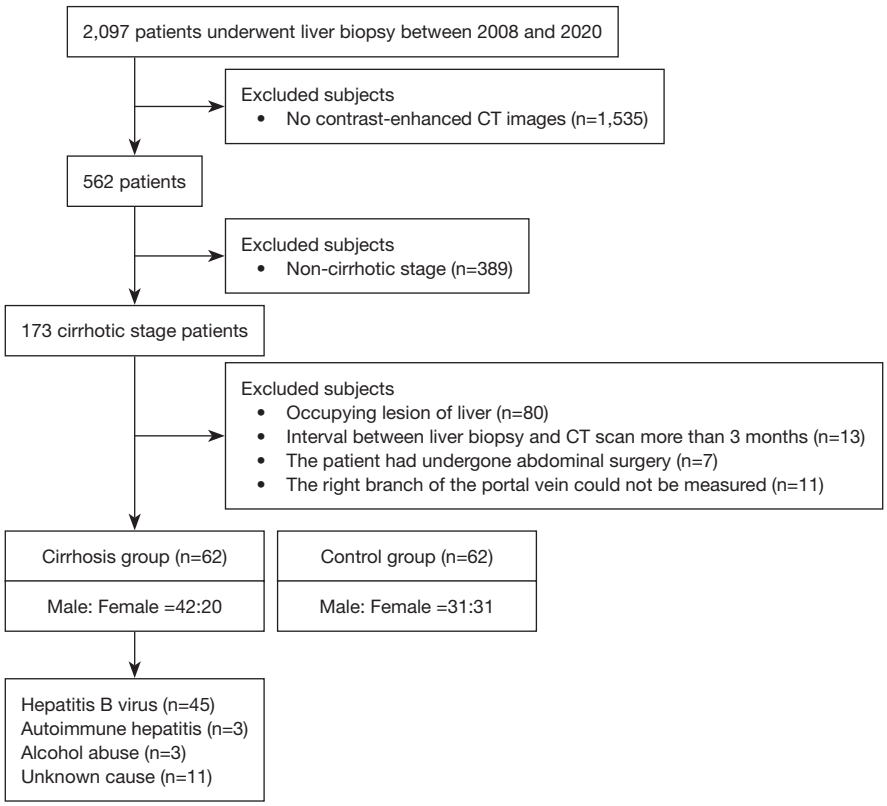

Figure 1 Patient population. Abdominal CT scans of 124 patients were retrospectively analysed. Included were 62 patients with cirrhosis and 62 patients without chronic liver disease. CT, computed tomography.

retrospective analysis was waived.

We conducted a retrospective analysis of 62 consecutive patients with pathologically diagnosed cirrhosis (cirrhosis group) and 62 individuals with no clinical evidence of chronic hepatic disease (control group) who underwent CT examination in Guangdong Provincial People's Hospital between August 2008 and August 2020. In the cirrhosis group, patients were pathologically diagnosed cirrhosis, but morphological changes, such as widening of liver fissures, wavy edges, enlargement of the caudate lobe and left lobe of the liver, and atrophy of the right lobe on imaging, were not sufficient to diagnose cirrhosis. Those who were pathologically confirmed to be free of cirrhosis and fibrosis and without a history of chronic hepatic were classified as the control group. For all included patients, the interval between the time of the liver biopsy and the abdominal contrast-enhanced CT scan was less than 3 months. The exclusion criteria were as follows: (I) the right branch of the portal vein could not be measured (for example, because of variation in the origin of the right portal vein); (II) the diameter of benign lesions in the liver was greater than 20 mm; (III) the image was blurred; (IV) the patient was under the age of 18 years; and (V) the patient had undergone abdominal surgery (*Figure 1*). The sample size for the analysis was based on the availability of CT images.

Pathological evaluation

First, the safest and best intercostal spaces were selected using CT or US, and percutaneous liver biopsy was performed after routine disinfection and induction of local anesthesia. Liver biopsy specimens were fixed with formaldehyde solution and embedded in paraffin, and the sections were stained with hematoxylin-eosin and elastic van Gieson. Each biopsy specimen was analyzed by a pathologist with more than 3 years' experience. The pathologists used the Knodell histology activity index scoring system, which considers periportal plus or minus bridging necrosis, intralobular degeneration and focal necrosis, portal inflammation, and fibrosis (21). On microscopy, the liver samples exhibited fibroblasts in the portal area showing evident hyperplasia, widening of the fibrous septum, grid

division in liver cells, the formation of a pseudo-lobule of the liver, and typical liver fibrosis; all of these findings are indicative of hepatic cirrhosis. Biopsy is the gold standard for the diagnosis of liver cirrhosis.

Imaging techniques

A General Electric Company (GE) Lightspeed VCT 64-slice spiral CT scanner (GE Healthcare, Chicago, IL, USA) was used to perform a non-contrast scan and an enhanced scan of the axial upper abdomen or the whole abdomen. The scanning parameters were as follows: 120 kVp; automatic tube current modulation; section thickness, 5 mm; and reconstruction section thickness, 1.0 mm. Following unenhanced CT, dynamic contrast enhancement was performed for 30 seconds (arterial phase), 60 seconds (portal phase), and 180 seconds (delayed phase) after the completion of an intravenous injection of nonionic contrast material (iopamidol 370 mg I/mL, 1.5 mL/kg) at a rate of 3.5–4.5 mL/s.

Measurement of the two evaluation methods

In this study, two distance ratio-based evaluation methods—our proposed L-distance ratio and the traditional caudate-right lobe ratio—were assessed and compared for the diagnosis of cirrhosis. Both methods were performed during the portal phase of enhanced CT scans. The detailed procedures for the two methods are presented below:

For L-distance ratio evaluation, two lines were first drawn parallel to the right branch. Then, two vertical lines were drawn at the bifurcation of the right branch and from the bifurcation of the right branch to the posterior edge of the liver, defined as R and to the anterior edge of the liver, defined as L. The L-distance ratio, named after its L-shape, was expressed as the ratio of R to L (*Figure 2A,2B*).

For the traditional caudate-right lobe ratio, lines I, II, and III were parallel to the midsagittal plane. Lines I, II, and III were drawn through the right lateral margin, the bifurcation of the right branch, and the outer edge of the caudate lobe, respectively. The distance between lines II and III (representing the width of the caudate lobe) was defined as C, and the distance between lines II and I (representing the width of the right lobe) was defined as R. The caudate-right lobe ratio was expressed as the ratio of C to R (*Figure 2C,2D*). All abdominal CT images were reviewed by two expert radiologists, each with more than 3 years' experience. The L-distance ratio and the caudate-right lobe ratio were measured using the described methods. Images of each patient were reviewed by evaluators, who were blinded to all patient information, including the final diagnosis.

Texture feature extraction

For each patient, a 30 mm^2 region of liver parenchyma was delineated in one slide using the ITK-SNAP software (version 4.7.2; https://itk.org/), and the region could not include blood vessels. Feature extraction was performed with the radiomics toolbox (22). Two types of quantitative image features were extracted: (I) histogram features (mean, variance, skewness, kurtosis, and moment 5–10); and (II) texture features [gray-level co-occurrence matrix (GLCM) energy, GLCM contrast, GLCM entropy, GLCM homogeneity, GLCM correlation, GLCM sumaverage, GLCM variance, GLCM dissimilarity, and GLCM autocorrelation]. The AUC value for distinguishing the cirrhosis and control groups was calculated for histogram and texture features. If the AUC value of a feature was greater than 0.70, the feature was considered potentially significant.

Statistical analysis

Intraclass correlation coefficients (ICCs) were used to analyze the interobserver agreement between the two observers. Binary logistic regression was used for univariate analysis. The strength of an association was given as an odds ratio (OR) with a 95% confidence interval (CI). The sensitivity, specificity, and accuracy of two methods for diagnosing cirrhosis were calculated at different cut-off points. To compare the L-distance ratio and the caudate-right lobe ratio, the ROC curve was constructed and the AUC calculated. The diagnostic value was determined by the AUC. The AUC values of the two methods were compared using the DeLong test. We also analyzed the distribution of normal and cirrhosis cases according to the prediction of the two methods. Patients with missing data were excluded, and the imputation method was not used in the analysis. All statistical analyses were performed with SPSS 26.0 (IBM Corp., Armonk, NY, USA) or R language (R version 4.0.3; R Foundation for Statistical Computing, Vienna, Austria), with a two-sided P value <0.05 indicating statistical significance.

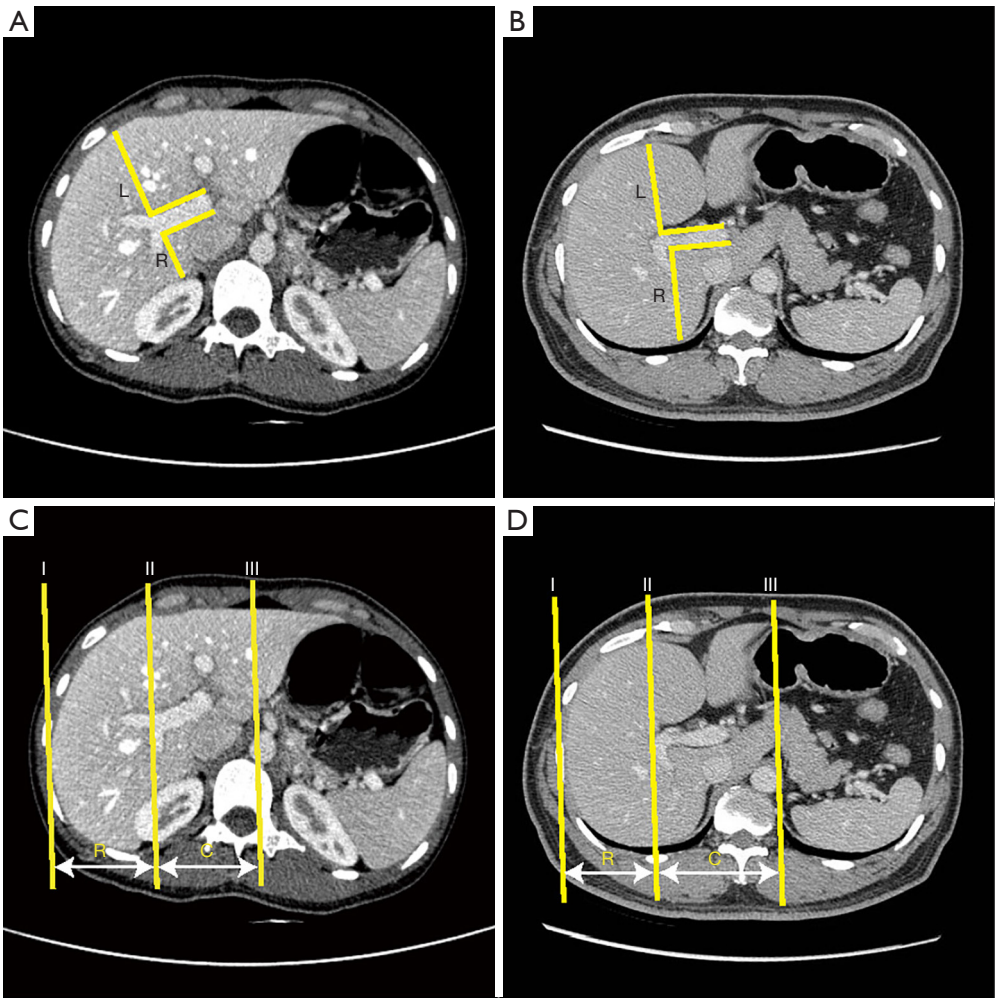

Figure 2 Definition of the two methods. (A) L-distance ratio evaluation: two lines were drawn parallel to the right branch. Two vertical lines were drawn at the bifurcation of the right branch from them to the posterior edge of the liver, defined as R, and to the anterior edge of the liver, defined as L. The L-distance ratio was expressed as the ratio of R to L. (B) The ratio calculated using L-distance ratio was 1.02 in this patient with cirrhosis. (C) Caudate-right lobe ratio evaluation: lines I, II, and III were parallel to the midsagittal plane. Line I was drawn through the right lateral margin; line II was drawn through the bifurcation of the right branch; and line III was drawn through the outer edge of the caudate lobe. The distance between lines II and III was defined as C, and the distance between lines II and I was defined as R. The caudate-right lobe ratio was expressed as the ratio of C to R. (D) The ratio calculated using the caudate-right lobe ratio was 1.34 in this patient with cirrhosis. L: the distance from the bifurcation of the right branch to the anterior edge of the liver; R: the distance from the bifurcation of the right branch to the posterior edge of the liver (A,B); the distance between lines II and I (C,D); C: the distance between lines II and III.

Results

Patients

The cirrhosis group included 42 men and 20 women (age range, 28–77 years; mean age, 51 years). The etiologies of cirrhosis included HBV infection (n=45), autoimmune hepatitis (n=3), alcohol abuse (n=3), or undetermined causes (n=11). The control group included 31 men and 31 women (age range, 29–75 years; mean age, 51 years). The mean histological activity index for the cirrhosis group was 10±2.6.

Consistency analysis

For the L-distance ratio, a high level of agreement was observed between the two radiologists (ICC =0.916, 95% CI: 0.884–0.940). A slightly lower ICC value was observed

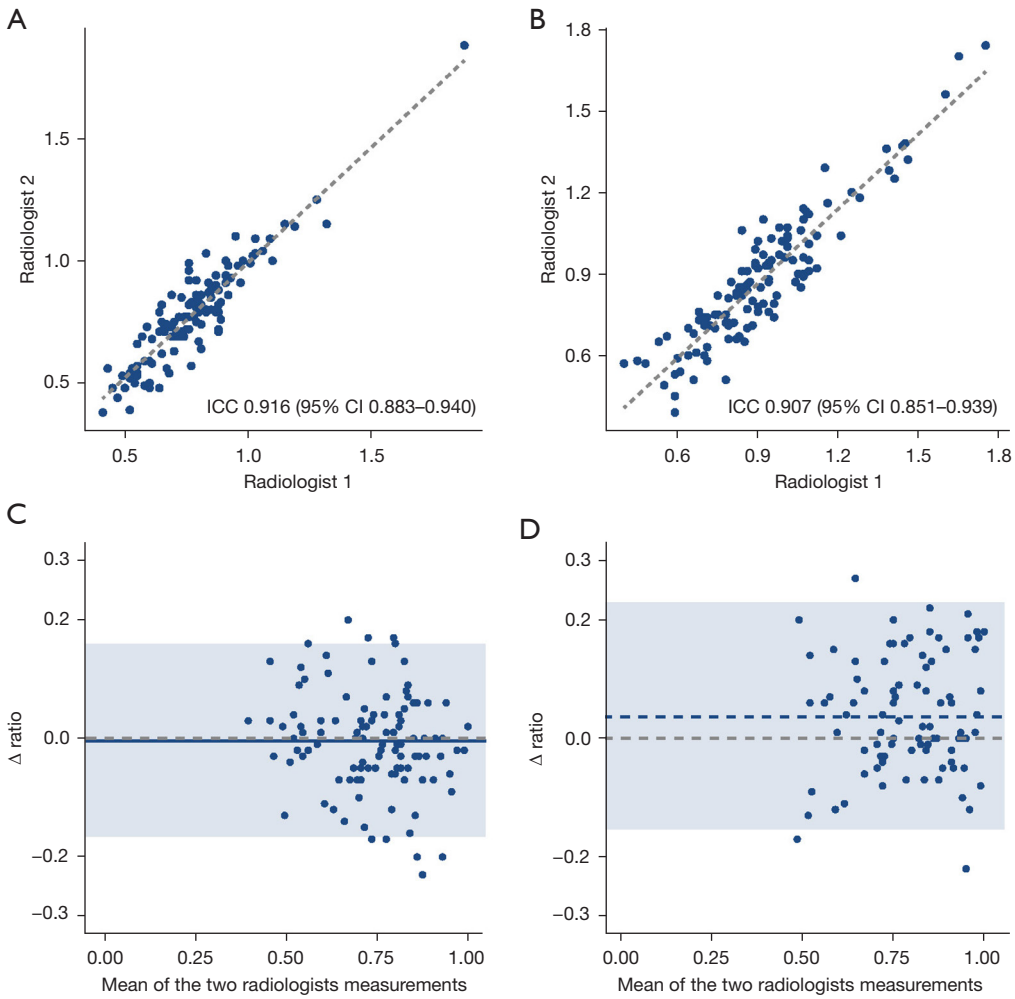

Figure 3 L-distance ratio and caudate-right lobe ratio consistency analysis. Concordance between two radiologists for the L-distance ratio (A) and the caudate-right lobe ratio (B). Bland-Altman plot for the two radiologists for the L-distance ratio (C) and the caudate-right lobe ratio (D). The solid horizontal line is the mean, the dashed line is zero, and the shaded regions are the 95% CIs. ICC, intraclass correlation coefficients; CI, confidence interval.

for the caudate-right lobe ratio (0.907, 95% CI: 0.851–0.939). The measurement results are presented as scatter plots in *Figure 3A,3B*. The Bland-Altman plot showed good agreement between the two radiologists for the L-distance ratio (*Figure 3C*), and the mean ratio difference between the two radiologists was –0.005 (95% CI: –0.166 to 0.157). For the caudate-right lobe ratio, the mean ratio difference was much further away from the zero-line, and the 95% CI was much broader (0.037, 95% CI: –0.154 to 0.227; *Figure 3D*).

Discrimination performance evaluation

The mean L-distance ratio was higher in the cirrhosis group than the control group (0.88±0.20 *vs.* 0.69±0.14, P<0.05), and the same trend was observed for the mean caudate-right lobe ratio (0.98±0.26 *vs.* 0.82±0.17, P<0.05). Using the median value of the L-distance ratio, patients were divided into high- and low-ratio groups. Logistic regression analysis showed that a high ratio was associated with cirrhosis (OR 6.47, 95% CI: 2.96–14.2, P<0.001). The analysis was also performed for the caudate-right lobe ratio method and produced a similar result (OR 2.89, 95% CI: 1.39–6.00, P=0.004).

The ROC curves of the two methods for diagnosing cirrhosis are shown in *Figure 4*. The discrimination performance of the L-distance ratio was superior to that of the caudate-right lobe ratio (AUC, 0.823 *vs.* 0.663,

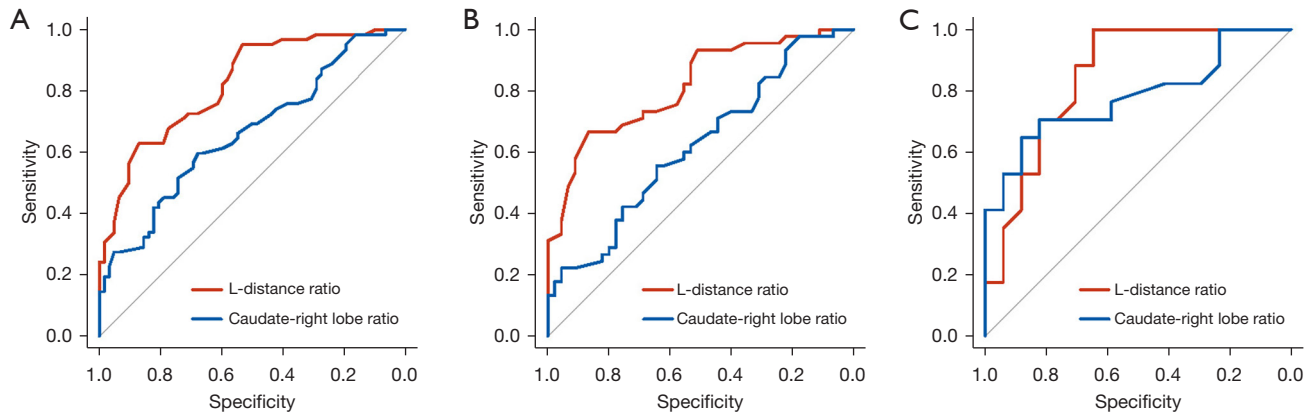

Figure 4 Receiver operating characteristic curves for the L-distance ratio and the caudate-right lobe ratio measured by radiologist 1. (A). ROC of all cases; (B) ROC of HBV group; (C) ROC of non-HBV group. ROC, receiver operating characteristic; HBV, hepatitis B virus.

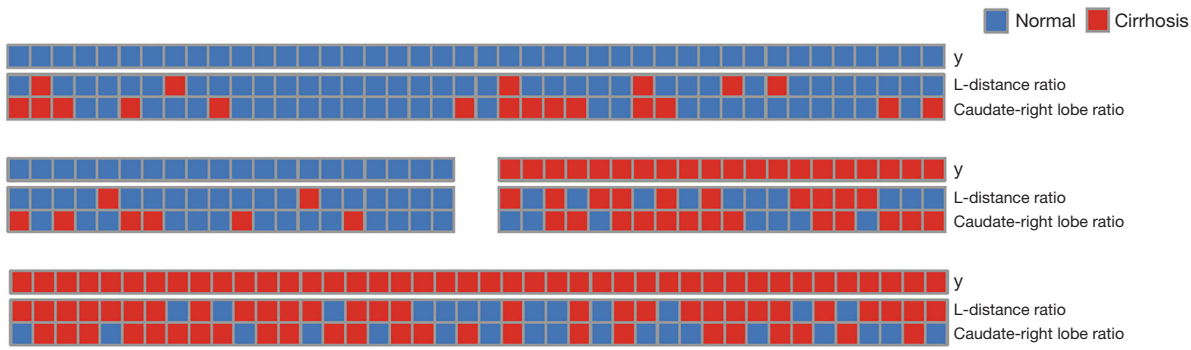

Figure 5 Distribution of normal and cirrhosis cases (y) predicted with the two methods.

P<0.05; *Figure 4A*). The optimal cut-off was selected at the ROC curve point with the joint maximum sensitivity and specificity values (Youden index). The cutoff point for the L-distance ratio was 0.825, and the accuracy, sensitivity, and specificity were 75.0%, 62.9%, and 87.1%, respectively. The threshold for the caudate-right lobe ratio was set as 0.915, and the accuracy, sensitivity, and specificity were 64.5%, 30.7%, and 98.4%, respectively. In the control group, 4.8% of cases were misjudged by both methods, and 59.7% were judged correctly. The proportion of cases judged incorrectly was lower with the L-distance ratio than with the caudate-right lobe ratio (8.1% *vs.* 27.4%). In the cirrhosis group, 14.5% of cases were misjudged by both methods, and 37.1% were judged correctly. Like in the control group, the proportion of cases judged incorrectly was lower with the L-distance ratio than with the caudate-right lobe ratio (22.6% *vs.* 25.8%; *Figure 5*).

We also divided the cirrhosis group into an HBV group (n=45) and non-HBV group (n=17) according to etiology. We found that the L-distance ratio had a better discrimination performance than did the caudate-right lobe ratio in both groups (AUC of HBV group: 0.815 *vs.* 0.620; AUC of non-HBV group: 0.848 *vs.* 0.782; *Figure 4B*,*4C*, *Table 1*). This result shows that our method is a stable tool for cirrhosis diagnosis.

Texture feature analysis

A total of 19 quantitative image features were extracted, and the AUCs of texture features are shown in Table S1. The AUC values of GLCM_contrast, GLCM_homogeneity, GLCM_correlation, and GLCM_dissimilarity were 0.74 (95% CI: 0.65–0.83), 0.73 (0.63–0.82), 0.76 (0.67–0.85), and 0.74 (0.65–0.83), respectively. As the above AUC values were all greater than 0.70, these features were considered significant.

Table 1 The areas under the receiver operating characteristic curves for the L-distance ratio and the caudate-right lobe ratio measured by radiologist 1 in three groups

Groups	AUC (95% CI)	
	L-distance ratio	Caudate-right lobe ratio
All	0.823 (0.752–0.894)	0.663 (0.569–0.757)
HBV group	0.815 (0.729–0.901)	0.620 (0.506–0.735)
Non-HBV group	0.848 (0.717–0.979)	0.782 (0.626–0.938)

AUC, area under the receiver operating characteristic curve; CI, confidence interval; HBV, hepatitis B virus.

Discussion

In this study, we proposed a new distance ratio-based quantification method, the L-distance ratio, for the accurate diagnosis of cirrhosis using enhanced CT images. Compared with the traditional caudate-right lobe ratio method, our proposed method is simple, accurate and robust, and has potential value in the diagnosis of cirrhosis.

Liver fibrosis causes compression and irregular stenoses of the intrahepatic branches of the portal vein (23), and as a result, the blood supply transitions from the portal vein to the hepatic artery (24,25). The blood supply to the right lobe has more influence usually because the right portal vein enters the right lobe directly (23). These events lead to morphological changes, including enlargement of the caudate and left liver lobes, and atrophy of the right lobe (26,27). Although these shape features have been used for the diagnosis of many tumors in clinical practice (28), using appearance alone to diagnose cirrhosis is subjective. Moreover, these features indicate that the disease has already progressed to a more severe stage. The treatment and prognosis of liver cirrhosis mainly depend on the stage of fibrosis (29), and there is a progressive increase in the relative risk of liver mortality with the development of fibrosis (30). Therefore, early screening of patients with cirrhosis is of great significance to guiding clinical treatment decisions.

To date, the diagnostic efficacy of two-dimensional diameter assessment in cirrhosis has not been satisfactory, and a recognized diagnostic standard has yet to be established. Cirrhosis typically manifests as hypertrophy in the left and caudate lobes and as atrophy of the right lobe (31). Based on these morphological changes, Harbin *et al.* (32) chose the main portal vein as a boundary marker to separate the caudate lobe from the right lobe and to calculate the ratio of their distances. When the cutoff point was 0.55, the accuracy was 65.7%. However, hypertrophy of the caudate lobe may extend further to the right, beyond the main portal vein, which may correspond to the bifurcation point of the right portal vein. Therefore, the right portal vein may be more suitable than the main portal vein for dividing the caudate lobe from the liver. Based on this, Awaya *et al.* (18) selected the bifurcation point of the right portal vein as the boundary marker and calculated the caudate-right lobe ratio. When the cutoff point was 0.9, the sensitivity, specificity, and accuracy were 71.7%, 77.4%, and 74.2%, respectively. The caudate lobe is composed of the left Spiegel lobe, the paracaval portion, and the caudate process, and their hemodynamics are generally variable (20), which also makes the degree of caudate lobe hypertrophy variable. Also, we found that the right branch bifurcation point was not at the same level as the caudate lobe, which influenced the diagnostic performance of the caudate-right lobe ratio. Research has shown that shrinkage in the anterior part of the right lobe, especially the middle hepatic vein drainage area, and enlargement of the posterior segment of the right lobe, are characteristic of hepatitis C-related cirrhotic liver (31,33). The right portal vein divides into anterior and posterior branches; the right anterior branch supplies segments V and VIII, while the right posterior branch supplies segments VI and VII (34).

In this study, we used the ratio of the vertical distance from the bifurcation point of the right portal vein to the sides of the liver and selected the most appropriate cutoff point to explore whether this method is effective in diagnosing cirrhosis. Our results show that the diagnostic efficacy of the L-distance ratio is superior to that that of the caudate-right lobe ratio. A high L-distance ratio was identified as an indicator for diagnosing cirrhosis (OR =6.47, 95% CI: 2.96–14.2, P<0.001). The AUC of our method reached 0.823, whereas that of the existing method was 0.663. However, the sensitivity of the caudate-right lobe ratio method at the optimal cutoff point in our study was lower than that reported by Awaya (18). A possible reason for this difference is that the primary etiology in the sample reported by Awaya was alcoholic cirrhosis. In another study, the proportion of patients with caudate lobe enlargement was significantly higher among those with alcoholic cirrhosis than among those with viral cirrhosis (P<0.001) (19). In the present study, cirrhosis was mostly caused by HBV, and alcoholic cirrhosis accounted for only three cases. Many studies have been conducted on the clinical impact of fibroscan and US elastography in the evaluation of hepatic

fibrosis, and these techniques have been reported to have higher accuracy than ratios measured on CT images (35). For example, the AUC of shear-wave elastography in the assessment of advanced fibrosis was 0.89, and cutoffs of 8.7 and 10.3 kPa provided sensitivity and specificity of 90% (17,36). However, a deliberate clinical approach informed by a knowledge of the pitfalls and preparation for multiple contingencies in case of indeterminate results is crucial. Our approach provides useful and complementary information for clinical practice.

Many studies have reported that texture features also achieved success in cirrhosis and hepatocellular carcinoma (37,38). We found that the AUC values of GLCM_contrast, GLCM_homogeneity, GLCM_correlation, and GLCM_dissimilarity were all greater than 0.70, but these features had a poorer performance than the L-distance ratio in our study. Although it may be better to combine the features, feature selection is usually not effective in studies with limited cases due to the issue of overfitting. Further studies using a larger cohort are needed to evaluate the performance of combing texture and morphology-based ratio features.

The measurements in this study did not require post-processing of the images and had high clinical operability. Additionally, the L-distance ratio method does not require the right branch to be at the same level as the caudate lobe, which compensates for the limitations of the caudate-right lobe ratio method. However, our study still had some limitations. First, as a single-center retrospective study, selection bias was inherent. Second, anatomical variation of the portal vein is present in approximately 20–35% of the population. The two common variations are trifurcation of the portal vein—where the portal vein divides into the right anterior, right posterior, and left branches—and early branching of the right posterior portal vein from the main portal vein. Another, less common, variation is early division of the right portal vein (34). Patients with this variation were excluded from the study, and consequently, there may have been a selection bias. Third, fact that we used a small sample from a single hospital was another limitation. We will require a large number of samples to demonstrate the advantages of our method in the future.

In conclusion, the proposed L-distance ratio can evaluate cirrhosis more accurately than the traditional caudate-right lobe ratio. This method is a non-invasive, convenient, and reproducible clinical measurement approach, and thus, provides value in guiding clinical treatment of cirrhosis. In patients with chronic liver disease, an L-distance ratio of more than 0.80 indicates that cirrhosis is likely, which could assist clinicians in formulating corresponding interventions to improve prognosis as much as possible.

Acknowledgments

Funding: This work was supported by Key-Area Research and Development Program of Guangdong Province (No. 2021B0101420006), the National Key R&D Program of China (No. 2021YFF1201003), the National Science Fund for Distinguished Young Scholars (No. 81925023), National Natural Science Foundation of China (No. 82071892), High-level Hospital Construction Project (Nos. DFJH201805, DFJHBF202105), Guangdong Provincial Key Laboratory of Artificial Intelligence in Medical Image Analysis and Application (No. 2022B1212010011) and the Natural Science Foundation of Guangdong Province (No. 2022A1515011252).

Footnote

Reporting Checklist: The authors have completed the STARD reporting checklist. Available at https://qims.amegroups.com/article/view/10.21037/qims-22-861/rc

Conflicts of Interest: All authors have completed the ICMJE uniform disclosure form (available at https://qims.amegroups.com/article/view/10.21037/qims-22-861/coif). The authors have no conflicts of interest to declare.

Ethical Statement: The authors are accountable for all aspects of the work in ensuring that questions related to the accuracy or integrity of any part of the work are appropriately investigated and resolved. The study was conducted in accordance with the Declaration of Helsinki (as revised in 2013). This retrospective study was approved by the institutional review board of Guangdong Provincial People's Hospital, and individual consent for this retrospective analysis was waived.

References

1. The global, regional, and national burden of cirrhosis by cause in 195 countries and territories, 1990-2017: a systematic analysis for the Global Burden of Disease Study 2017. Lancet Gastroenterol Hepatol 2020;5:245-66.
2. Moon AM, Singal AG, Tapper EB. Contemporary Epidemiology of Chronic Liver Disease and Cirrhosis. Clin Gastroenterol Hepatol 2020;18:2650-66.
3. Paik JM, Golabi P, Younossi Y, Mishra A, Younossi ZM. Changes in the Global Burden of Chronic Liver Diseases From 2012 to 2017: The Growing Impact of NAFLD. Hepatology 2020;72:1605-16.
4. Virzì A, Gonzalez-Motos V, Tripon S, Baumert TF, Lupberger J. Profibrotic Signaling and HCC Risk during Chronic Viral Hepatitis: Biomarker Development. J Clin Med 2021;10:977.
5. Vo Quang E, Shimakawa Y, Nahon P. Epidemiological projections of viral-induced hepatocellular carcinoma in the perspective of WHO global hepatitis elimination. Liver Int 2021;41:915-27.
6. Li M, Wang ZQ, Zhang L, Zheng H, Liu DW, Zhou MG. Burden of Cirrhosis and Other Chronic Liver Diseases Caused by Specific Etiologies in China, 1990-2016: Findings from the Global Burden of Disease Study 2016. Biomed Environ Sci 2020;33:1-10.
7. Shi Y, Zheng M. Hepatitis B virus persistence and reactivation. BMJ 2020;370:m2200.
8. Xiao J, Wang F, Wong NK, He J, Zhang R, Sun R, Xu Y, Liu Y, Li W, Koike K, He W, You H, Miao Y, Liu X, Meng M, Gao B, Wang H, Li C. Global liver disease burdens and research trends: Analysis from a Chinese perspective. J Hepatol 2019;71:212-21.
9. Fattovich G, Bortolotti F, Donato F. Natural history of chronic hepatitis B: special emphasis on disease progression and prognostic factors. J Hepatol 2008;48:335-52.
10. Campos-Murguía A, Ruiz-Margáin A, González-Regueiro JA, Macías-Rodríguez RU. Clinical assessment and management of liver fibrosis in non-alcoholic fatty liver disease. World J Gastroenterol 2020;26:5919-43.
11. Hsu C, Caussy C, Imajo K, Chen J, Singh S, Kaulback K, Le MD, Hooker J, Tu X, Bettencourt R, Yin M, Sirlin CB, Ehman RL, Nakajima A, Loomba R. Magnetic Resonance vs Transient Elastography Analysis of Patients With Nonalcoholic Fatty Liver Disease: A Systematic Review and Pooled Analysis of Individual Participants. Clin Gastroenterol Hepatol 2019;17:630-637.e8.
12. Larrey D, Meunier L, Ursic-Bedoya J. Liver Biopsy in Chronic Liver Diseases: Is There a Favorable Benefit: Risk Balance? Ann Hepatol 2017;16:487-9.
13. Neuberger J, Patel J, Caldwell H, Davies S, Hebditch V, Hollywood C, Hubscher S, Karkhanis S, Lester W, Roslund N, West R, Wyatt JI, Heydtmann M. Guidelines on the use of liver biopsy in clinical practice from the British Society of Gastroenterology, the Royal College of Radiologists and the Royal College of Pathology. Gut 2020;69:1382-403.
14. Di Tommaso L, Spadaccini M, Donadon M, Personeni N, Elamin A, Aghemo A, Lleo A. Role of liver biopsy in hepatocellular carcinoma. World J Gastroenterol 2019;25:6041-52.
15. Lurie Y, Webb M, Cytter-Kuint R, Shteingart S, Lederkremer GZ. Non-invasive diagnosis of liver fibrosis and cirrhosis. World J Gastroenterol 2015;21:11567-83.
16. Moreno C, Mueller S, Szabo G. Non-invasive diagnosis and biomarkers in alcohol-related liver disease. J Hepatol 2019;70:273-83.
17. Tapper EB, Loomba R. Noninvasive imaging biomarker assessment of liver fibrosis by elastography in NAFLD. Nat Rev Gastroenterol Hepatol 2018;15:274-82.
18. Awaya H, Mitchell DG, Kamishima T, Holland G, Ito K, Matsumoto T. Cirrhosis: modified caudate-right lobe ratio. Radiology 2002;224:769-74.
19. Ozaki K, Matsui O, Kobayashi S, Minami T, Kitao A, Gabata T. Morphometric changes in liver cirrhosis: aetiological differences correlated with progression. Br J Radiol 2016;89:20150896.
20. Mao W, Jiang X, Cao Y, Xiong S, Huang Y, Jiao L, Wang HJ. A practical study of the hepatic vascular system anatomy of the caudate lobe. Quant Imaging Med Surg 2021;11:1313-21.
21. Desmet VJ. Knodell RG, Ishak KG, Black WC, Chen TS, Craig R, Kaplowitz N, Kiernan TW, Wollman J. Formulation and application of a numerical scoring system for assessing histological activity in asymptomatic chronic active hepatitis [Hepatology 1981;1:431-435]. J Hepatol 2003;38:382-6.
22. Vallières M, Freeman CR, Skamene SR, El Naqa I. A radiomics model from joint FDG-PET and MRI texture features for the prediction of lung metastases in soft-tissue sarcomas of the extremities. Phys Med Biol 2015;60:5471-96.
23. Chen XL, Chen TW, Zhang XM, Li ZL, Zeng NL, Li T, Wang D, Li J, Fang ZJ, Li H, Chen J, Liu J, Xu GH, Ren J, Wu JL, Li CP. Quantitative assessment of the presence and

severity of cirrhosis in patients with hepatitis B using right liver lobe volume and spleen size measured at magnetic resonance imaging. PLoS One 2014;9:e89973.
24. Prin M, Bakker J, Wagener G. Hepatosplanchnic circulation in cirrhosis and sepsis. World J Gastroenterol 2015;21:2582-92.
25. Wang D, Chen TW, Zhang XM, Li J, Zeng NL, Li L, Tang YL, Huang YC, Li R, Chen F, Chen YL. Liver Lobe Based Multi-Echo Gradient Recalled Echo T2*-Weighted Imaging in Chronic Hepatitis B-Related Cirrhosis: Association with the Presence and Child-Pugh Class of Cirrhosis. PLoS One 2016;11:e0154545.
26. Wells ML, Moynagh MR, Carter RE, Childs RA, Leitch CE, Fletcher JG, Yeh BM, Venkatesh SK. Correlation of hepatic fractional extracellular space using gadolinium enhanced MRI with liver stiffness using magnetic resonance elastography. Abdom Radiol (NY) 2017;42:191-8.
27. Tan GX, Miranda R, Sutherland T. Causes of hepatic capsular retraction: a pictorial essay. Insights Imaging 2016;7:831-40.
28. Wang H, Xu Z, Zhang H, Huang J, Peng H, Zhang Y, Liang C, Zhao K, Liu Z. The value of magnetic resonance imaging-based tumor shape features for assessing microsatellite instability status in endometrial cancer. Quant Imaging Med Surg 2022;12:4402-13.
29. Baues M, Dasgupta A, Ehling J, Prakash J, Boor P, Tacke F, Kiessling F, Lammers T. Fibrosis imaging: Current concepts and future directions. Adv Drug Deliv Rev 2017;121:9-26.
30. Taylor RS, Taylor RJ, Bayliss S, Hagström H, Nasr P, Schattenberg JM, Ishigami M, Toyoda H, Wai-Sun Wong V, Peleg N, Shlomai A, Sebastiani G, Seko Y, Bhala N, Younossi ZM, Anstee QM, McPherson S, Newsome PN. Association Between Fibrosis Stage and Outcomes of Patients With Nonalcoholic Fatty Liver Disease: A Systematic Review and Meta-Analysis. Gastroenterology 2020;158:1611-1625.e12.
31. Soufi M, Otake Y, Hori M, Moriguchi K, Imai Y, Sawai Y, Ota T, Tomiyama N, Sato Y. Liver shape analysis using partial least squares regression-based statistical shape model: application for understanding and staging of liver fibrosis. Int J Comput Assist Radiol Surg 2019;14:2083-93.
32. Harbin WP, Robert NJ, Ferrucci JT Jr. Diagnosis of cirrhosis based on regional changes in hepatic morphology: a radiological and pathological analysis. Radiology 1980;135:273-83.
33. Ozaki K, Matsui O, Kobayashi S, Sanada J, Koda W, Minami T, Kawai K, Gabata T. Selective atrophy of the middle hepatic venous drainage area in hepatitis C-related cirrhotic liver: morphometric study by using multidetector CT. Radiology 2010;257:705-14.
34. Madhusudhan KS, Vyas S, Sharma S, Srivastava DN, Gupta AK. Portal vein abnormalities: an imaging review. Clin Imaging 2018;52:70-8.
35. Yang L, Ling W, He D, Lu C, Ma L, Tang L, Luo Y, Chen S. Shear wave-based sound touch elastography in liver fibrosis assessment for patients with autoimmune liver diseases. Quant Imaging Med Surg 2021;11:1532-42.
36. Cassinotto C, Boursier J, de Lédinghen V, Lebigot J, Lapuyade B, Cales P, Hiriart JB, Michalak S, Bail BL, Cartier V, Mouries A, Oberti F, Fouchard-Hubert I, Vergniol J, Aubé C. Liver stiffness in nonalcoholic fatty liver disease: A comparison of supersonic shear imaging, FibroScan, and ARFI with liver biopsy. Hepatology 2016;63:1817-27.
37. Yang ZX, Liang HY, Hu XX, Huang YQ, Ding Y, Yang S, Zeng MS, Rao SX. Feasibility of histogram analysis of susceptibility-weighted MRI for staging of liver fibrosis. Diagn Interv Radiol 2016;22:301-7.
38. Qiu Q, Duan J, Duan Z, Meng X, Ma C, Zhu J, Lu J, Liu T, Yin Y. Reproducibility and non-redundancy of radiomic features extracted from arterial phase CT scans in hepatocellular carcinoma patients: impact of tumor segmentation variability. Quant Imaging Med Surg 2019;9:453-64.

Cite this article as: Ye H, Wang Q, Huang H, Zhao K, Li P, Liu Z, Wang G, Liang C. L-distance ratio: a new distance ratio-based evaluation method for the diagnosis of cirrhosis using enhanced computed tomography. Quant Imaging Med Surg 2023;13(3):1499-1509. doi: 10.21037/qims-22-861

Supplementary

Table S1 Areas under the receiver operating characteristic curves of texture features

Feature name	AUC (95% CI)
Mean	0.52 (0.42–0.63)
Variance	0.57 (0.46–0.67)
Skewness	0.54 (0.43–0.64)
Kurtosis	0.55 (0.44–0.65)
Moment5	0.54 (0.43–0.65)
Moment6	0.55 (0.44–0.65)
Moment7	0.52 (0.41–0.63)
Moment8	0.55 (0.45–0.66)
Moment9	0.51 (0.40–0.61)
Moment10	0.54 (0.44–0.65)
GLCM_energy	0.54 (0.43–0.64)
GLCM_contrast	0.74 (0.65–0.83)
GLCM_entropy	0.51 (0.40–0.62)
GLCM_homogeneity	0.73 (0.63–0.82)
GLCM_correlation	0.76 (0.67–0.85)
GLCM_sumaverage	0.51 (0.40–0.61)
GLCM_variance	0.52 (0.41–0.62)
GLCM_dissimilarity	0.74 (0.65–0.83)
GLCM_autocorrelation	0.54 (0.44–0.65)

AUC, the area under the receiver operating characteristic curve; CI, confidence interval; GLCM, gray-level co-occurrence matrix.

https://dx.doi.org/10.21037/qims-22-861